Palaeobiodiversity and Palaeoenvironments (2019) 99:477–494
https://doi.org/10.1007/s12549-019-00384-5

SENCKENBERG

ORIGINAL PAPER

Conodont stratigraphy and conodont biofacies of the shallow-water Kuh-e-Bande-Abdol-Hossein section (SE Anarak, Central Iran)

Ali Bahrami[1] · Peter Königshof[2] · Hossein Vaziri-Moghaddam[1] · Bahareh Shakeri[1] · Iliana Boncheva[3]

Received: 23 May 2018 / Revised: 24 September 2018 / Accepted: 4 April 2019 / Published online: 24 July 2019
© Senckenberg Gesellschaft für Naturforschung and Springer-Verlag GmbH Germany, part of Springer Nature 2019

Abstract

The Middle to Upper Devonian Kuh-e-Bande-Abdol-Hossein section in eastern Central Iran is an overall shallow marine, nearshore to open marine facies setting that contains a highly variable conodont record generally characterised by an *Icriodid-Polygnathid* biofacies. The lithology and the palaeoenvironmental setting is similar to other localities in Central Iran and exhibits numerous hiatuses. A continuous biostratigraphic record could not be established, but the section preserves the Givetian/Frasnian boundary. Based on the conodont record, major gaps also occur in the Famennian which confirms earlier results reported from other sections of similar palaeoenvironments in Central Iran.

Keywords Upper Givetian · Frasnian · Conodont biofacies · Frasne-Event · Bahram Formation · Central Iran

Introduction

The late Middle and early Late Devonian represents a relatively warm period with an acme in diversity, size and latitudinal distribution of reefs and associated shallow-water sediments in the Middle Devonian (Flügel and Kiessling 2002; Joachimski et al. 2009). On the other hand, the mid-Palaeozoic underwent a dramatic change in Earth's climate systems which resulted in changes in ocean chemistry and sea level. As a consequence these palaeoecosystems were impacted by several mass extinctions and ecological perturbations spanning millions of years. Fluctuations in physical palaeoenvironments and resultant mass extinctions recorded in the sedimentological record by lithological changes and geochemical excursions which are also dependent on the depositional setting (Mottequin et al. 2017).

Middle to Late Devonian strata are mainly composed of shallow-water facies and occur in isolated units in Central Iran (e.g. Zahedi 1973; Soffel and Förster 1984; Wendt et al. 2005). In the frame of a scientific cooperation between the University of Isfahan, Islamic Republic of Iran, Geological Institute, Bulgarian Academy of Sciences and Senckenberg Research Institute and Natural History Museum Frankfurt, Germany, we have studied different sections in Central Iran in order to improve the biostratigraphic framework, mainly by conodonts, in Devonian to Carboniferous shallow-water palaeoenvironments (Bahrami et al. 2014a, b, 2015, 2018; Ernst et al. 2017; Königshof et al. 2017). Despite the difficulties to apply the pelagic conodont zonation (Klapper and Ziegler 1979; Ziegler and Sandberg 1990; Clausen et al. 1993) in shallow-water realms the generally rich conodont faunas (at least in distinct beds) in Central Iran allow the application of an alternative conodont zonation for the Givetian which was proposed by Narkiewicz and Bultynck (2007, 2010), Bultynck and Gouwy (2008) and Narkiewicz (2011). The biostratigraphic record is a prerequisite to trace and describe equivalent bioevent levels and/or sequence boundaries which occur in the shallow-water realms

✉ Ali Bahrami
Bahrami_geo@yahoo.com; a.bahrami@sci.ui.ac.ir

Peter Königshof
peter.koenigshof@senckenberg.de

Hossein Vaziri-Moghaddam
avaziri7304@gmail.com

Bahareh Shakeri
b.shakeri1835@gmail.com

Iliana Boncheva
boncheva2005@yahoo.com

[1] Department of Geology, Faculty of Science, University of Isfahan, Ishafan, Iran

[2] Senckenberg Research Institute and Natural History Museum Frankfurt, Senckenberganlage 25, 60325 Frankfurt am Main, Germany

[3] Geological Institute, Bulgarian Academy of Sciences, 113 Sofia, Bulgaria

(Königshof et al. 2016 and references therein). Detailed biostratigraphy provides the background for further studies as shown from the Zefreh section in Central Iran (Königshof et al. 2017). Furthermore, conodont biofacies analysis has the potential to reconstruct palaeoenvironmental changes which was applied in various papers in different stratigraphical units (e.g. Sandberg 1976; Weddige and Ziegler 1979; Sandberg and Dreesen 1984; Ziegler and Weddige 1999; Söte et al. 2017; Lüddeke et al. 2017) and may complete sedimentological and facies data even if species groups within genera may have had different palaeoecological distribution (Sandberg 1976; Corradini 1998; Lüddecke et al. 2017).

The Kuh-e-Bande-Abdol-Hossein section, which is located southeast of Anarak (Fig. 1), was first mentioned by Reyer and Mohafez (1970) and later examined in more detail by Sharkovski et al. (1984) and Wendt et al. (2005). We re-examined this section because it is mainly composed of sedimentary rocks ranging from Ordovician to Permian age (Hairapetian et al. 2015; Lensch and Davoudzadeh 1982). Herein we focus on the Middle to Upper Devonian strata in order to establish the biostratigraphic framework of this section by means of conodonts as a prerequisite for forthcoming studies on geochemistry, sedimentology and facies. Furthermore, we briefly discuss the conodont biofacies of the Kuh-e-Bande-Abdol-Hossein section and discuss the sections investigated earlier by us in Central Iran.

Geological setting

The Kuh-e-Bande-Abdol-Hossein section belongs to the Anarak-Khur Block and constitutes the Central-East Iran Microplate, which is composed of a complex 5000–8000-m-thick series of sedimentary, volcaniclastic and metamorphic rocks (Soffel et al. 1996; Aghanabati, 2010). According to Motaghi et al. (2015), Central Iran is relatively less deformed and surrounded by active margins. Marine sediments occur in northern and Central Iran ranging from the mid-Devonian into the Early Pennsylvanian (Bahrami et al. 2014a, b, 2018). During the Devonian, Central Iran was located in the low latitudes of the Palaeotethys at the northern margin of Gondwana (Berberian and King 1981, Scotese 2001). Most of the Middle and Upper Devonian rocks represent shallow-water sediments and exhibit palaeoenvironmental settings from open marine to supratidal settings (Königshof et al. 2017 and references therein). Due to different subsidence and/or horst and graben structures, up to 2000 m of siliciclastics, mainly shallow-water sediments were deposited in Central Iran (Wendt et al. 1997, 2002, 2005).

Ambient rocks of the Kuh-e-Bande-Abdol-Hossein section, are mainly composed of Late Palaeozoic sedimentary and metamorphic rocks (Houshmandzadeh 1977; Almasian 1997; Leven and Gorgij 2006; Fig. 1). For instance, the Lakh marble is regarded as the uppermost unit of the Anarak metamorphics

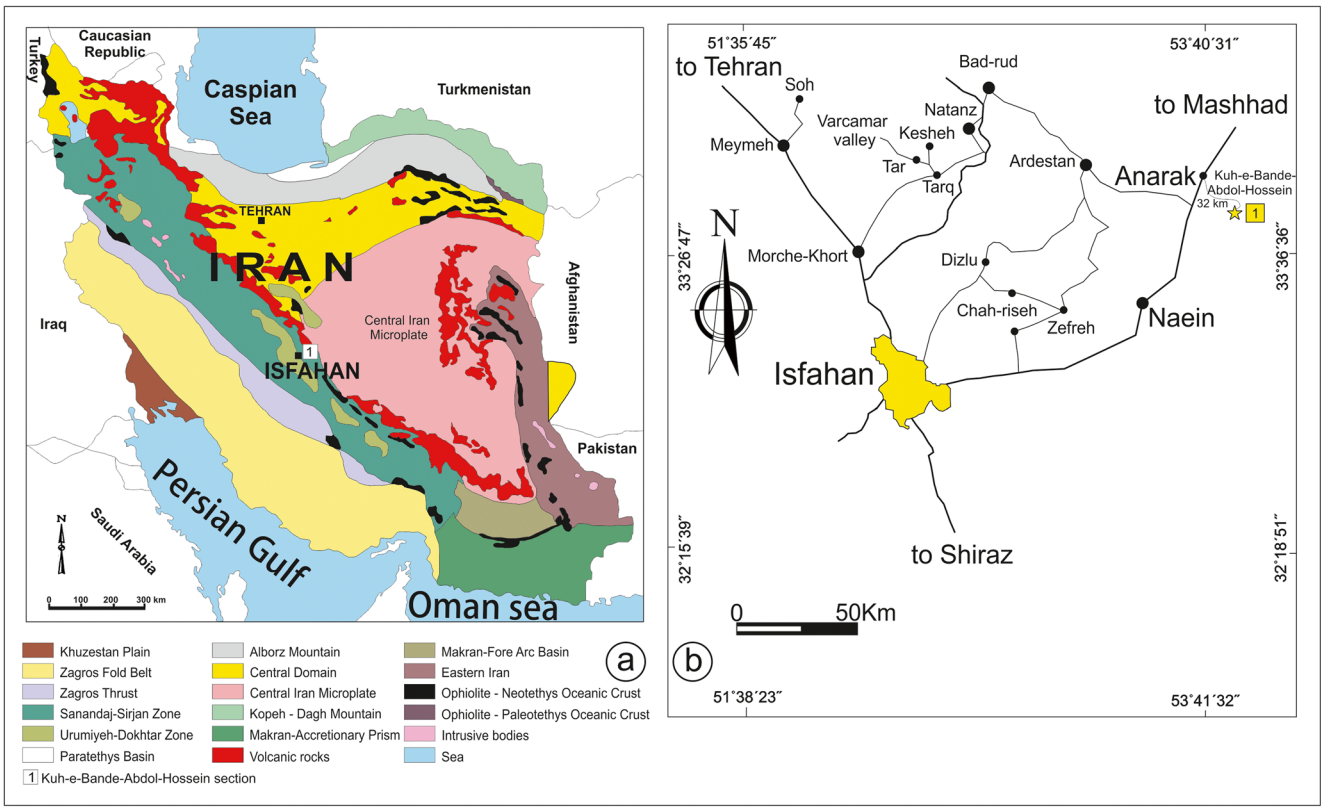

Fig. 1 **a** Position of the section in Central Iran; **b** road map showing the position of the Kuh-e-Bande-Abdol-Hossein section northeast of Isfahan (modified after Bakhtiari 2005)

and is of early Cambrian age (Sharkovski et al. 1984). These marbles are unconformably overlain by unmetamorphosed Palaeozoic sediments of Kuh-e-Bande-Abdol-Hossein section located approximately 32 km southeast of Anarak and 180 km northeast of Isfahan (E 53° 52′ 55″ and N 33° 10′ 90″ WGS coordinates; Fig. 1). The entire section has a thickness of approximately 1200 m, ranging stratigraphically from the Ordovician (Shirgesht Formation) to the Permian (Jamal Formation; Hairapetian et al. 2015; Lensch and Davoudzadeh 1982). The sequence comprises of some hiatuses due to erosion and/or tectonic activity. In this paper, we will concentrate on Middle and Late Devonian sediments of the Kuh-e-Bande-Abdol-Hossein section which belongs to the Bahram Formation (Fig. 2).

Material and methods

In order to improve the biostratigraphy of the Kuh-e-Bande-Abdol-Hossein section, 78 conodont samples of approximately 2 to 3 kg each were taken from the carbonates and processed by conventional methods using 10% formic acid. Washed residues were sieved and separated into three fractions, and conodonts were handpicked utilising a microscope. Depending on the depositional facies setting, the number of conodonts per sample is highly variable, e.g. in dolostones no conodonts where found whereas in shallow-water limestones a good number of species occurred in distinct beds. A total number of 2050 conodonts were obtained from the residues which led to the identification of 41 species and subspecies within six genera. The conventional conodont biofacies model was applied according to different authors (e.g. Sandberg 1976; Ziegler and Sandberg 1984; Sandberg and Dreesen 1984; Ziegler and Weddige 1999). Lithological differences were described based on field observations. Conodonts described herein are stored at the University of Isfahan, IR of Iran.

Lithology of the Kuh-e-Bande-Abdol-Hossein section

The fossiliferous Middle Devonian part of the Kuh-e-Bande-Abdol-Hossein section is covered by Upper Devonian siliciclastic rocks of the Padeha Formation which are composed of an alternation of quartzitic sandstones, shales and dolostones with intercalated basalt flows (Wendt et al. 2005). The latter ones can reach a thickness of 60 m whereas the entire formation is approximately 290 m thick. This unit is continuously overlain by the Sibzar Formation. The uppermost part of the Sibzar Formation has a thickness of 48 m and is composed of thick-bedded microbial dolostones (Fig. 3). The next younger Bahram Formation starts with an alternation of dolostones and dolomitic limestones and has a thickness of 335 m. Due to lithological differences observed in the field, the Bahram Formation in the Kuh-e-Bande-Abdol-Hossein section was subdivided into 14 units (Fig. 3).

The first 56-m-thick unit (Sh1–S20; Fig. 3) is composed of thick-bedded, partly laminated dolomitic limestones with rare fossil content (Fig. 4a, b). The following unit is 94 m thick and is composed of medium to thick-bedded fossiliferous (rugose corals, stromatoporoids, bryozoans, brachiopods) limestones (Fig. 4c, d). At the base of unit 2, the first conodonts were found (Fig. 3). At the top of this unit, *Ancyrodella* cf. *pristina* was found which indicate the Givetian/Frasnian boundary. The level slightly above the proposed G/F boundary is characterised by abrupt lithological changes and points to a rapid deepening. The calcareous unit is conformably overlain by greenish shales which have a thickness of 5.5 m (unit 3, Fig. 4e). The overlaying unit (sample numbers S114.5–S145) is composed of mainly shallow-water bioclastic wackestones. Conodonts were found only at the base of this unit (Fig. 3). The shallow-water limestones are overlain by an alternation of thin-bedded limestones and shales (unit 5, sample numbers S145–S159) followed by medium-bedded limestones of unit 6 (sample number S159–S177; Fig. 3). The next unit (unit 7, sample numbers S177–S209) has a thickness of 32 m. It is composed of alternating shales and fossiliferous limestones and shows a gradual transition from thin-bedded to medium-bedded limestones of unit 8 (sample numbers S232–S239). Unit 9 is composed of thin reddish shales at the base and at the top with intercalated limestones and has a thickness of 7 m. This unit is overlain by grey carbonates of various thicknesses (unit 10, sample numbers S239–S261; Fig. 3). The next two units (unit 11 and unit 12), which belong to the Frasnian, show a gradual transition from medium to thick-bedded, fossiliferous limestones. Intercalated are marls and sandy limestones. The thickness of both units is 26 m. Below the Frasnian/Famennian boundary limestones are thick-bedded and the facies points to more shallow-water palaeoenvironments (unit 13, Fig. 3) with numerous fossils such as brachiopods, bryozoans and stromatoporoids. It is difficult to provide definite conodont substage levels due to the lack of sufficient zonal index conodonts (see section biostratigraphy). Units 10 to 13 cover the upper *rhenana* to *linguiformis* zones but there was no indication of event layers revealed in the sedimentological record such as black shales or limestones. Observed sea level changes (T–R trends based on the sedimentological record) in that part of the section are confirmed by changes in the conodont biofacies (see relevant section). According to conodont stratigraphy, we place the Frasnian/Famennian boundary around sample number S310 at the base of unit 14 (Fig. 3). The top of the described section (middle and upper part of unit 14) consists of 25 m of red marls which are disconformably overlain by greenish or reddish nodular limestones (Sardar Formation) of Carboniferous age (Fig. 4f).

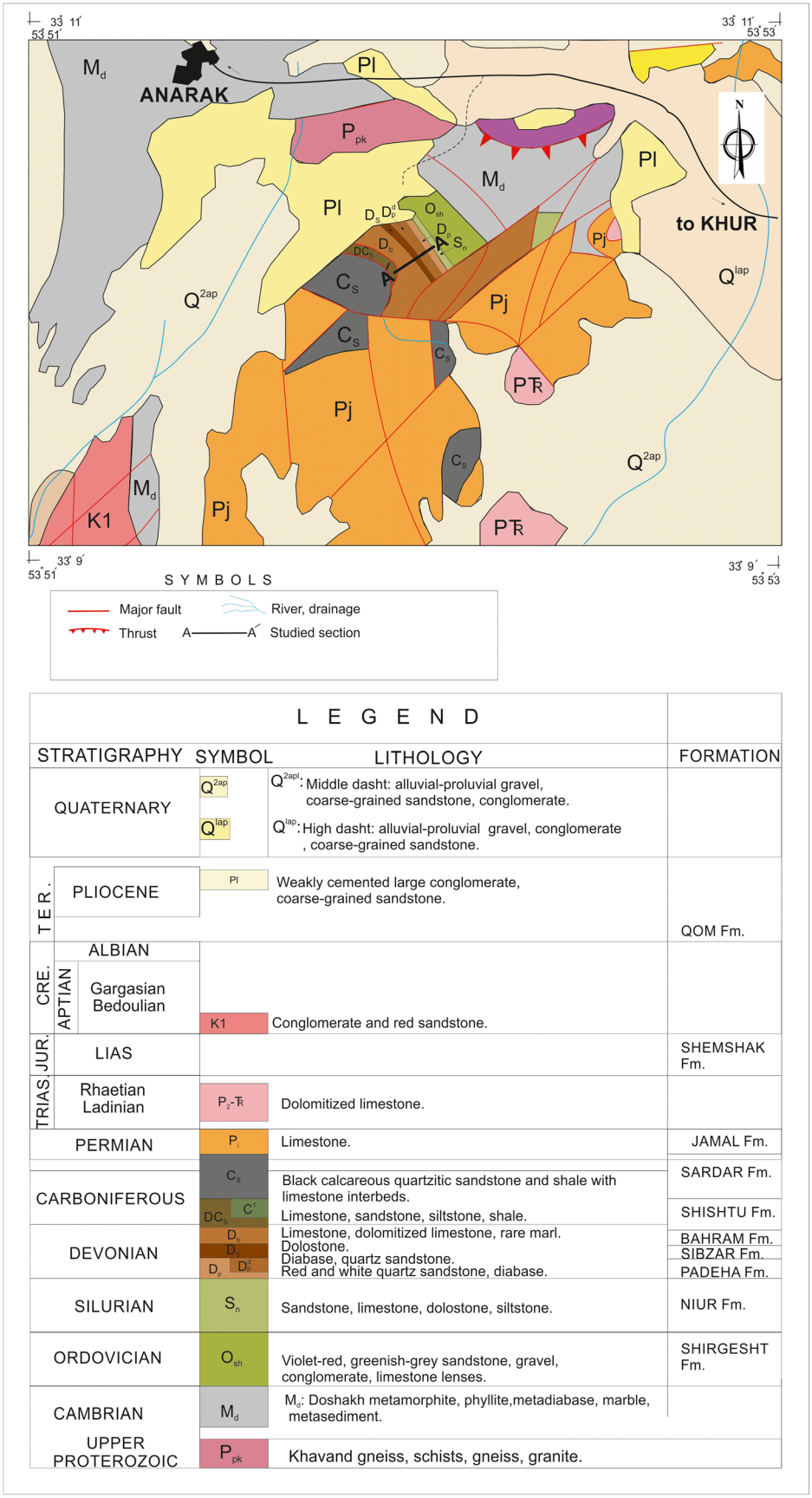

Fig. 2 Geological map and location of the investigated section A`—A (from Sharkovski et al. 1984)

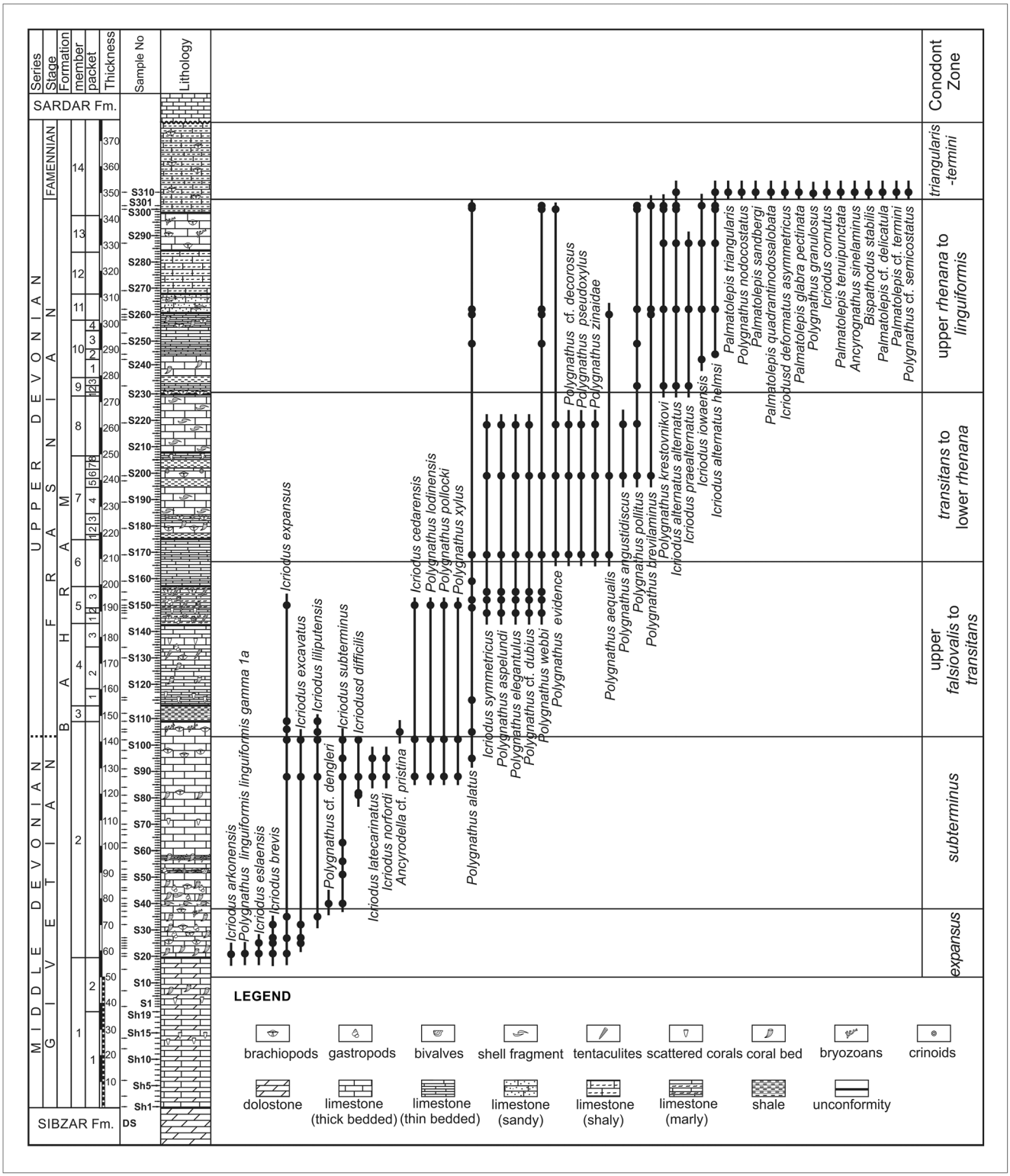

Fig. 3 Lithology and conodont stratigraphy of the Middle to Late Devonian Kuh-e-Bande-Abdol-Hossein section. Please note that in the right column, the *Icriodus expansus* and the *Icriodus subterminus* conodont zones represent shallow-water facies setting (Bultynck 1987; Bultynck and Gouwy 2008; Narkiewicz and Bultynck 2007, 2010; Narkiewicz 2011), whereas the others represent the Standard Conodont Zonation (Klapper and Ziegler 1979; Clausen et al. 1993)

Conodonts found in the last 10 m exhibit a very wide stratigraphical range, from the *termini* to *gracilis expansa* zones which supports the assumption by Wendt et al. (2005) that there is a major gap in the Famennian.

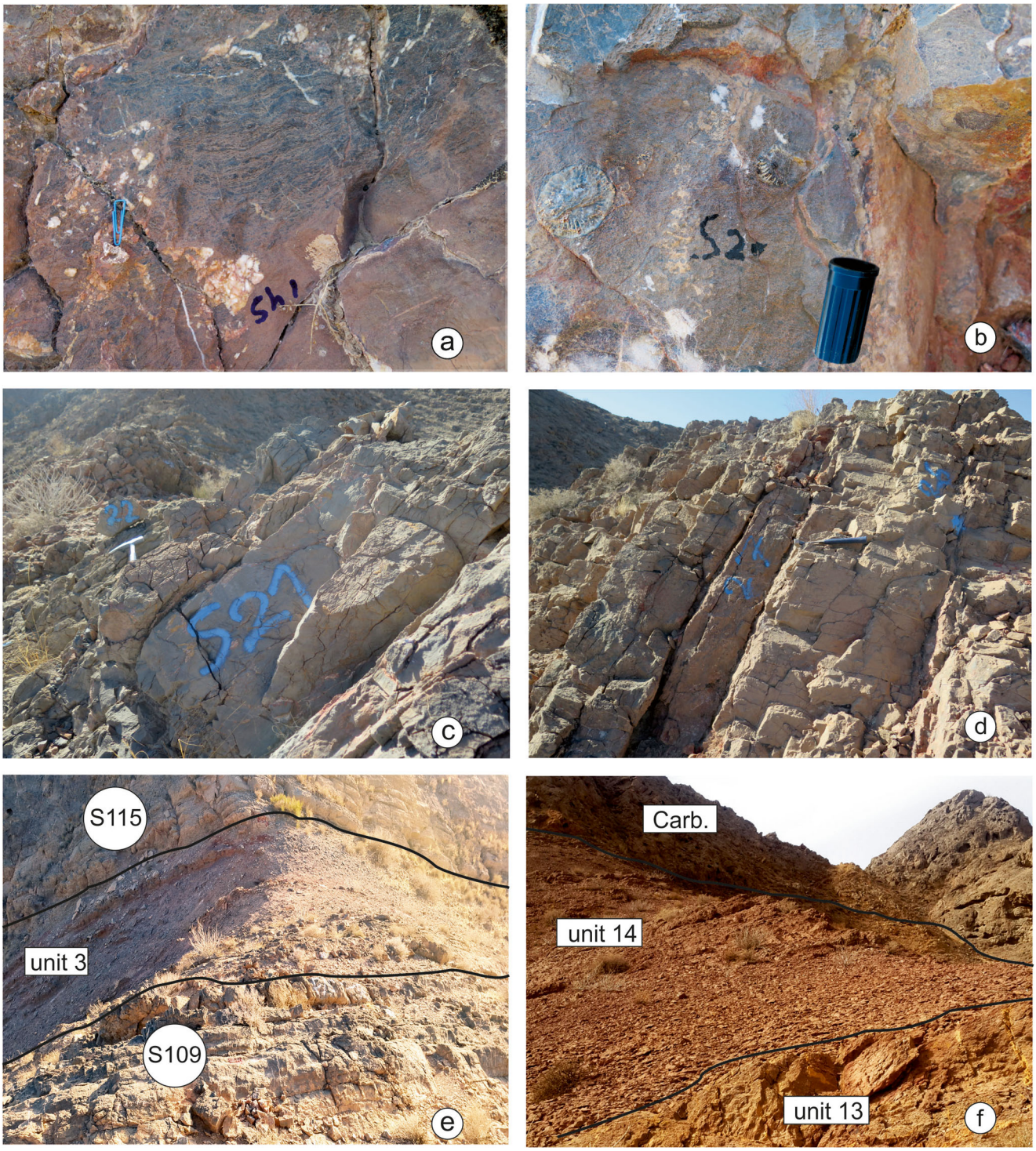

Fig. 4 Lithology of some portions of the Kuh-e-Bande-Abdol-Hossein section: **a**, **b** thick-bedded, partly dolomitic limestone at the base of the section; **c**, **d** fossiliferous limestone in the Givetian (*expansus* Zone); **e** marly limestone overlain by greenish shales at the Givetian/Frasnian boundary (unit 3) **f** units 13 and 14 of the section

Conodont succession

Conodont faunas from the Kuh-e-Bande-Abdol-Hossein section (Figs. 5, 6 and 7) are dominated by species of *Icriodus* and *Polygnathus* in the Givetian and Frasnian and *Icriodus*, *Polygnathus* and *Palmatolepis* in the Famennian. *Ancyrodella*, *Ancyrognathus* and *Bispathodus* are accessory elements. The conodont succession is described in the stratigraphical order, from the oldest samples to the youngest samples.

Based on the overall shallow-water setting of the section, an alternative conodont zonation (see Narkiewicz and Bultynck 2007, 2010; Bultynck and Gouwy 2008; Narkiewicz 2011) was applied for the Givetian. According to the studied samples, six conodont zones were identified:

expansus Zone

First conodonts were found in limestones in the uppermost part of unit 1 and the *expansus* Zone covers the interval from sample S11–S37. The lower boundary of *expansus* Zone is defined by the first appearance of *Icriodus expansus* Branson and Mehl, 1938 (Narkiewicz and Bultynck 2010) and the upper boundary corresponds to the first appearance of *Icriodus subterminus* Youngquist, 1947; the first occurrence of this species represents the lower boundary of the subsequent biozone (Sandberg and Dreesen 1984; Narkiewicz and Bultynck 2007, 2010; Bultynck and Gouwy 2008). The accompanying conodont association in this biozone contains the following species: *Polygnathus linguiformis linguiformis γ 1a*, *Icriodus eslaensis*, *Icriodus excavatus*, *Icriodus brevis*, *Icriodus expansus*, *Icriodus arkonensis*, *Icriodus lilliputensis.*

subterminus Zone

The interval of the *subterminus* Zone ranges from sample S38–S103. The lower boundary of the *subterminus* Zone corresponds to the first occurrence of *Icriodus subterminus* Youngquist, 1947 (Narkiewicz and Bultynck, 2007, 2010; Bultynck and Gouwy 2008) and the upper boundary coincides with the first appearance of *Ancyrodella pristina* (Klapper and Lane, 1985). Other accompanying conodonts in the *subterminus* Zone are the following: *Icriodus excavatus*, *Icriodus expansus*, *Icriodus cedarensis*, *Icriodus lilliputensis*, *Polygnathus xylus*, *Polygnathus pollocki*, *Polygnathus alatus*, *Polygnathus lodinensis*, *Icriodus difficilis*, *Icriodus norfordi* and *Icriodus latecarinatus.*

Upper *falsiovalis* to *transitans* zones

This 63-m-thick interval covers the samples S102–S167 and conodont diversity increases. The lower boundary of the biozone corresponds to the first occurrence of *Ancyrodella pristina* (Klapper and Lane, 1985). The upper boundary of this biozone coincides to the first appearance of *Polygnathus aequalis* Klapper and Lane, 1985 in the *transitans* Zone (Ziegler and Sandberg 1996); the first presence of this species represents the lower boundary of the subsequent biozone.

According to the range of *Ancyrodella pristina*, its occurrence indicates the Givetian-Frasnian boundary in our section as the first appearance of *Ancyrodella pristina* marks the beginning of the Late Devonian (Sandberg et al. 1989). The first appearance of *Ancyrodella* cf. *Ad. pristina* corresponds with the first thin-bedded limestones just below greyish shales where we place the Givetian/Frasnian boundary (Fig. 3). This conodont association contains taxa which have a stratigraphical range from the Givetian to the Late Devonian such as *Icriodus excavatus*, *Icriodus expansus* and *Polygnathus angustidiscus*, but the appearance of *Polygnathus xylus*, *Polygnathus webbi*, *Polygnathus pollocki*, *Polygnathus lodinensis*, *Polygnathus elegantulus*, *Polygnathus aspelundi* and *Polygnathus* cf. *dubius* point to the upper part of lower Frasnian in the section (upper *falsiovalis* and *transitans* zones). The middle Frasnian *punctata*, *hassi* and *jamieae* zones are not documented in the section because of the lack of zonal index taxa, most probably due to hiatuses.

transitans to Upper *rhenana* zones

The conodont zones cover the sample interval from the middle part of unit 6 to the top of unit 8 (samples S168–S230). The lower boundary of this interval corresponds to the first occurrence of *Polygnathus aequalis* Klapper and Lane, 1985 in the *transitans* Zone (Ziegler and Sandberg, 1996). The upper boundary of this interval corresponds to the first occurrence of *Icriodus alternatus alternatus* Branson and Mehl, 1934 in the Upper *rhenana* Zone; the first appearance of this species represents the lower boundary of subsequent biozone (Ji and Ziegler 1993). Other conodonts of this interval are the following: *Polygnathus alatus*, *Polygnathus webbi*, *Polygnathus brevilaminus*, *Polygnathus politus*, *Polygnathus pseudoxylus*, *Polygnathus* cf. *decororosus* and *Polygnathus zinaidae.*

Upper *rhenana* to *linguiformis* zones

The lower boundary of the next interval, which ranges from samples S230–S300, corresponds to the first appearance of *Icriodus alternatus alternatus* Branson and Mehl, 1934 in the Upper *rhenana* Zone (Ji and Ziegler 1993) and the upper boundary of this biozone corresponds to the last occurrence of *Polygnathus politus* Ovanatanova, 1969; *Polygnathus webbi* Stauffer, 1938; *Polygnathus alatus* Huddle, 1934; *Polygnathus evidens* Klapper and Lane, 1985 in the *linguiformis* Zone (Ziegler and Sandberg 1996). The last appearance of these species represents the lower boundary of the subsequent biozone. Accompanying conodonts found in this interval are the following: *Polygnathus alatus*, *Polygnathus webbi*, *Polygnathus politus*, *Polygnathus aequalis*, *Polygnathus evidens*, *Polygnathus brevilaminus*, *Icriodus alternatus helmsi*, *Icriodus alternatus alternatus* and *Icriodus iowaensis.*

triangularis to *termini* zones

This 10-m-thick biozone involves specimens determined in samples S300 to S310. The lithology of this biozone is characterised by an alternation of red marls with interlayers of limestone. The lower boundary of this biozone

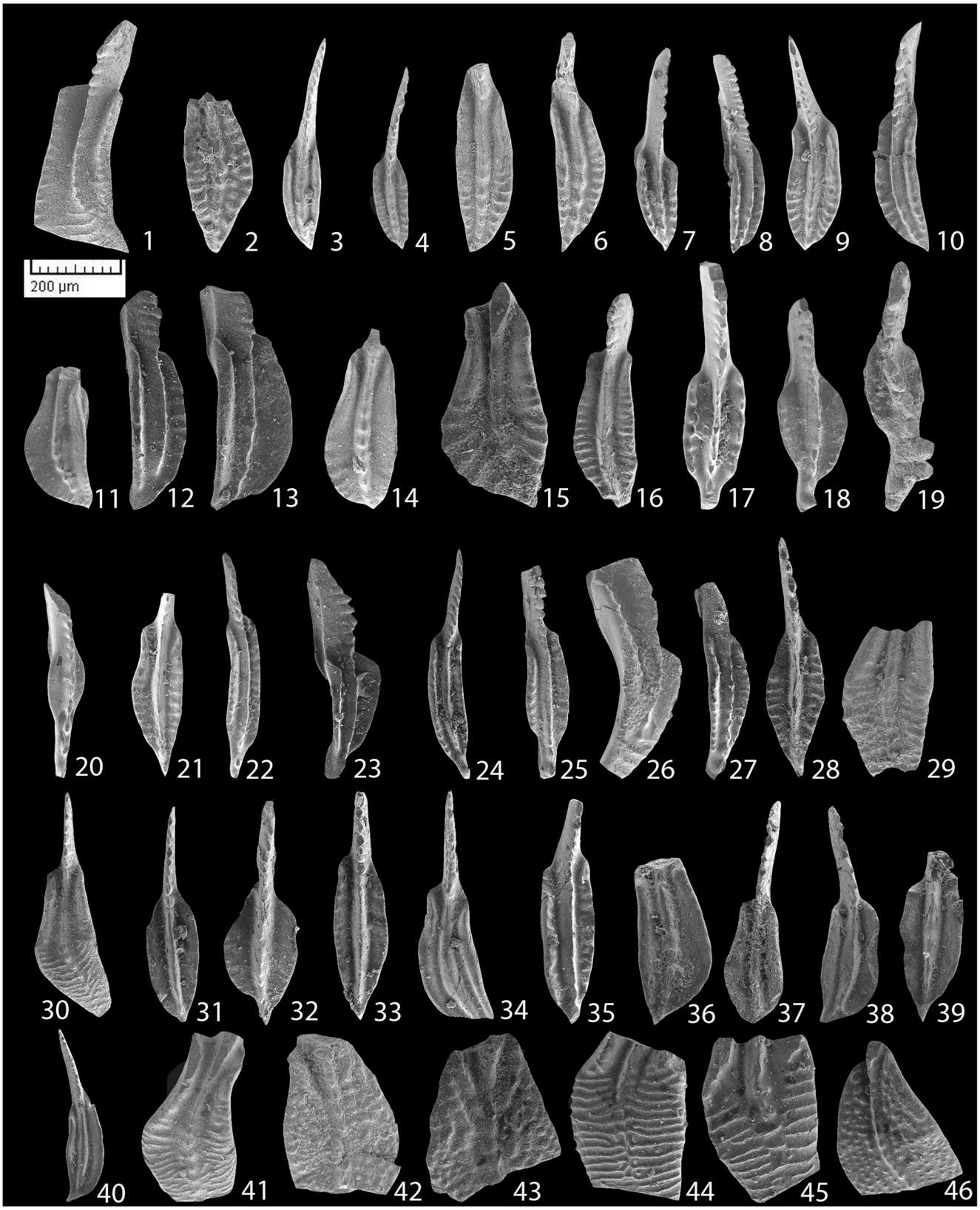

corresponds to the last presence of *Polygnathus politus*, Ovanatanova, 1969; *Polygnathus webbi*, Stauffer, 1938; *Polygnathus alatus*, Huddle, 1934; *Polygnathus evidens*, Klapper and Lane, 1985 and the first appearance of

◀ **Fig. 5** **1** *Polygnathus linguiformis linguiformis* Hinde, 1879 γ1a morphotype; upper view, Kuh-e-Bande-Abdol-Hossein (SE Anarak) section, northeast Isfahan, EUIC 100, sample S21, × 40. **2** *Polygnathus* cf. *P. dengleri* Bischoff and Ziegler, 1957; upper view, Kuh-e-Bande-Abdol-Hossein (SE Anarak) section, northeast Isfahan, EUIC 101, sample S40, × 40. **3–6** *Polygnathus pseudoxylus* Kononova, Alekseev, Barskov and Reimers, 1996; **3** upper view, Kuh-e-Bande-Abdol-Hossein (SE Anarak) section, northeast Isfahan, EUIC 107, sample S169, × 40; **4** upper view, Kuh-e-Bande-Abdol-Hossein (SE Anarak) section, northeast Isfahan, EUIC 111, sample S199, × 40; **5** upper view, Kuh-e-Bande-Abdol-Hossein (SE Anarak) section, northeast Isfahan, EUIC 112, sample S199, × 40; **6** upper view, Kuh-e-Bande-Abdol-Hossein (SE Anarak) section, northeast Isfahan, EUIC 113, sample S199, × 40. **7–9** *Polygnathus xylus* Stauffer, 1940; **7** upper view, Kuh-e-Bande-Abdol-Hossein (SE Anarak) section, northeast Isfahan, EUIC 115, Sample S88, × 40; **8** upper view, Kuh-e-Bande-Abdol-Hossein (SE Anarak) section, northeast Isfahan, EUIC 117, sample S88, × 40; **9** upper view, Kuh-e-Bande-Abdol-Hossein (SE Anarak) section, northeast Isfahan, EUIC 135, sample S88, × 40. **10**, **12** *Polygnathus alatus* Huddle, 1934; **10** upper view, Kuh-e-Bande-Abdol-Hossein (SE Anarak) section, northeast Isfahan, EUIC 124, sample S95, × 40; **12** upper view, Kuh-e-Bande-Abdol-Hossein (SE Anarak) section, northeast Isfahan, EUIC 156, sample S301, × 40. **11**, **34** *Polygnathus aequalis* Klapper and Lane, 1985; **11** upper view, Kuh-e-Bande-Abdol-Hossein (SE Anarak) section, northeast Isfahan EUIC 131, sample S169, × 40; **34** upper view, Kuh-e-Bande-Abdol-Hossein (SE Anarak) section, northeast Isfahan, EUIC 180, sample S260, × 40; **13**, **14**, **36**, **37** *Polygnathus zinaidae* Kononova, Alekseev, Barskov and Reimers, 1996; **13** upper view, Kuh-e-Bande-Abdol-Hossein (SE Anarak) section, northeast Isfahan, EUIC 175, sample S199, ×40; **14** upper view, Kuh-e-Bande-Abdol-Hossein (SE Anarak) section, northeast Isfahan, EUIC 138, sample S169, × 40; **36** upper view, Kuh-e-Bande-Abdol-Hossein (SE Anarak) section, northeast Isfahan, EUIC 203, sample S169, × 40; **37** upper view, Kuh-e-Bande-Abdol-Hossein (SE Anarak) section, northeast Isfahan, EUIC 207, sample S219, × 40. **15** *Polygnathus webbi* Stauffer, 1938; upper view, Kuh-e-Bande-Abdol-Hossein (SE Anarak) section, northeast Isfahan, EUIC 178, sample S199, × 40. **16** *Polygnathus* cf. *dubius* Hinde, 1879; upper view, Kuh-e-Bande-Abdol-Hossein (SE Anarak) section, northeast Isfahan, EUIC 181, sample S199, × 40. **17**, **23** *Polygnathus brevilaminus* Branson and Mehl, 1934; **17** upper view, Kuh-e-Bande-Abdol-Hossein (SE Anarak) section, northeast Isfahan, EUIC 141, sample S301, × 40; **23** upper view, Kuh-e-Bande-Abdol-Hossein (SE Anarak) section, northeast Isfahan, EUIC 159, sample S260, × 40. **18–20** *Polygnathus angustidiscus* Youngquist, 1947; **18** upper view, Kuh-e-Bande-Abdol-Hossein (SE Anarak) section, northeast Isfahan, EUIC 142, sample S218, × 40; **19** upper view, Kuh-e-Bande-Abdol-Hossein (SE Anarak) section, northeast Isfahan, EUIC 143, sample S199, × 40; **20** upper view, Kuh-e-Bande-Abdol-Hossein (SE Anarak) section, northeast Isfahan EUIC 144, sample S199, × 40. **21** *Polygnathus* cf. *decorosus* Stauffer, 1938; upper view, Kuh-e-Bande-Abdol-Hossein (SE Anarak) section, northeast Isfahan, EUIC 148, sample S219, × 40. **22**, **24**, **25**, **27**, **35** *Polygnathus pollocki* Druce, 1976; **22** upper view, Kuh-e-Bande-Abdol-Hossein (SE Anarak) section, northeast Isfahan, EUIC 147, sample S88, × 40; **24** upper view, Kuh-e-Bande-Abdol-Hossein (SE Anarak) section, northeast Isfahan, EUIC 172, sample S102, × 40; **25** upper view, Kuh-e-Bande-Abdol-Hossein (SE Anarak) section, northeast Isfahan, EUIC 163, sample S150, × 40; **27** upper view, Kuh-e-Bande-Abdol-Hossein (SE Anarak) section, northeast Isfahan, EUIC 155, sample S102, × 40; **35** upper view, Kuh-e-Bande-Abdol-Hossein (SE Anarak) section, northeast Isfahan, EUIC 198, sample S150, × 40. **26** *Polygnathus* cf. *semicostatus* Branson and Mehl, 1934; upper view, Kuh-e-Bande-Abdol-Hossein (SE Anarak) section, northeast Isfahan, EUIC 149, sample S310, × 40. **28**, **33** *Polygnathus lodinensis* Posler, 1969; **28** upper view, Kuh-e-Bande-Abdol-Hossein (SE Anarak) section, northeast Isfahan, EUIC 170, sample S88, × 40; **33** upper view, Kuh-e-Bande-Abdol-Hossein (SE Anarak) section, northeast Isfahan, EUIC 167, sample S102, × 40. **29**, **30** *Polygnathus krestovnikovi* Ovnatanova, 1969; **29** upper view, Kuh-e-Bande-Abdol-Hossein (SE Anarak) section, northeast Isfahan, EUIC 152, sample S300, × 40; **30** upper view, Kuh-e-Bande-Abdol-Hossein (SE Anarak) section, northeast Isfahan, EUIC 177, sample S300, × 40. **31–32** *Polygnathus elegantulus* Klapper and Lane, 1985; **31** upper view, Kuh-e-Bande-Abdol-Hossein (SE Anarak) section, northeast Isfahan, EUIC 165, sample S218, × 40; **32** upper view, Kuh-e-Bande-Abdol-Hossein (SE Anarak) section, northeast Isfahan, EUIC 166, sample S199, × 40. **38** *Polygnathus aspelundi* Savage and Funai, 1980; **38** upper view, Kuh-e-Bande-Abdol-Hossein (SE Anarak) section, northeast Isfahan, EUIC 218, sample S218, × 40; **39**, **40** *Polygnathus politus* Ovnatanova, 1969; **39** upper view, Kuh-e-Bande-Abdol-Hossein (SE Anarak) section, northeast Isfahan, EUIC 209, sample S300, × 40; **40** upper view, Kuh-e-Bande-Abdol-Hossein (SE Anarak) section, northeast Isfahan, EUIC 218, sample S301, × 40. **41**, **44–45** *Polygnathus evidens* Klapper and Lane, 1985; **41** upper view, Kuh-e-Bande-Abdol-Hossein (SE Anarak) section, northeast Isfahan, EUIC 151, sample S300, × 40; **44** upper view, Kuh-e-Bande-Abdol-Hossein (SE Anarak) section, northeast Isfahan, EUIC 187, sample S218, × 40; **45** upper view, Kuh-e-Bande-Abdol-Hossein (SE Anarak) section, northeast Isfahan, EUIC 188, sample S199, × 40. **42–43** *Polygnathus nodocostatus* Branson and Mehl, 1934; **42** upper view, Kuh-e-Bande-Abdol-Hossein (SE Anarak) section, northeast Isfahan, EUIC 154, sample S310, × 40; **43** upper view, Kuh-e-Bande-Abdol-Hossein (SE Anarak) section, northeast Isfahan, EUIC 189, sample S310, × 40. **46** *Polygnathus granulosus* Muller and Muller, 1957; upper view, Kuh-e-Bande-Abdol-Hossein (SE Anarak) section, northeast Isfahan, EUIC 190, sample S310, × 40

Palmatolepis triangularis Sannemann, 1955a. Conodonts which occur in the Middle *termini*—Zone are *Palmatolepis termini*, *Polygnathus semicostatus* and *Icriodus alternatus helmsi*. The latter one became extinct at the top of this conodont zone.

Other conodonts found in this level of the section are *Icriodus iowaensis*, *Ancryognathus sinelamina*, *Bispathodus stabilis*, *Palmatolepis sandbergi*, *Palmatolepis tenuipunctata*, *Palmatolepis quadrantinodosalobata*, *Palmatolepis glabra pectinata*, *Icriodus alternatus alternatus*, *Polygnathus granulosus and Polygnathus nodocostatus.* This assemblage indicates even younger conodont zones, e.g. based on the occurrence of *Bispathodus stabilis*. According to the sedimentological record, this part is characterised by hiatuses and/or reworked sediments.

Conodont biofacies

Due to the variable shallow-water facies, conodonts found in the section exhibit different conodont biofacies. Thus, we applied the conventional conodont biofacies analysis (Sandberg 1976; Weddige and Ziegler 1979; Sandberg and Ziegler 1979; Sandberg and Dreesen 1984; Ziegler and Weddige 1999) and we discuss the genus-level approach with possible sea level changes based on the sedimentological record. The conodont biofacies record shows variations from *Icriodus*-dominated genera (*Icriodid-Polygnathid* biofacies) and *Polygnathus*-dominated genera (*Polygnathid-Icriodid* biofacies). Some specific layers exhibit up to 100% of these two genera (Fig. 8) and in distinct layers, other genera occur in low frequency, such as *Palmatolepis*, *Ancyrognathus*, *Ancyrodella*

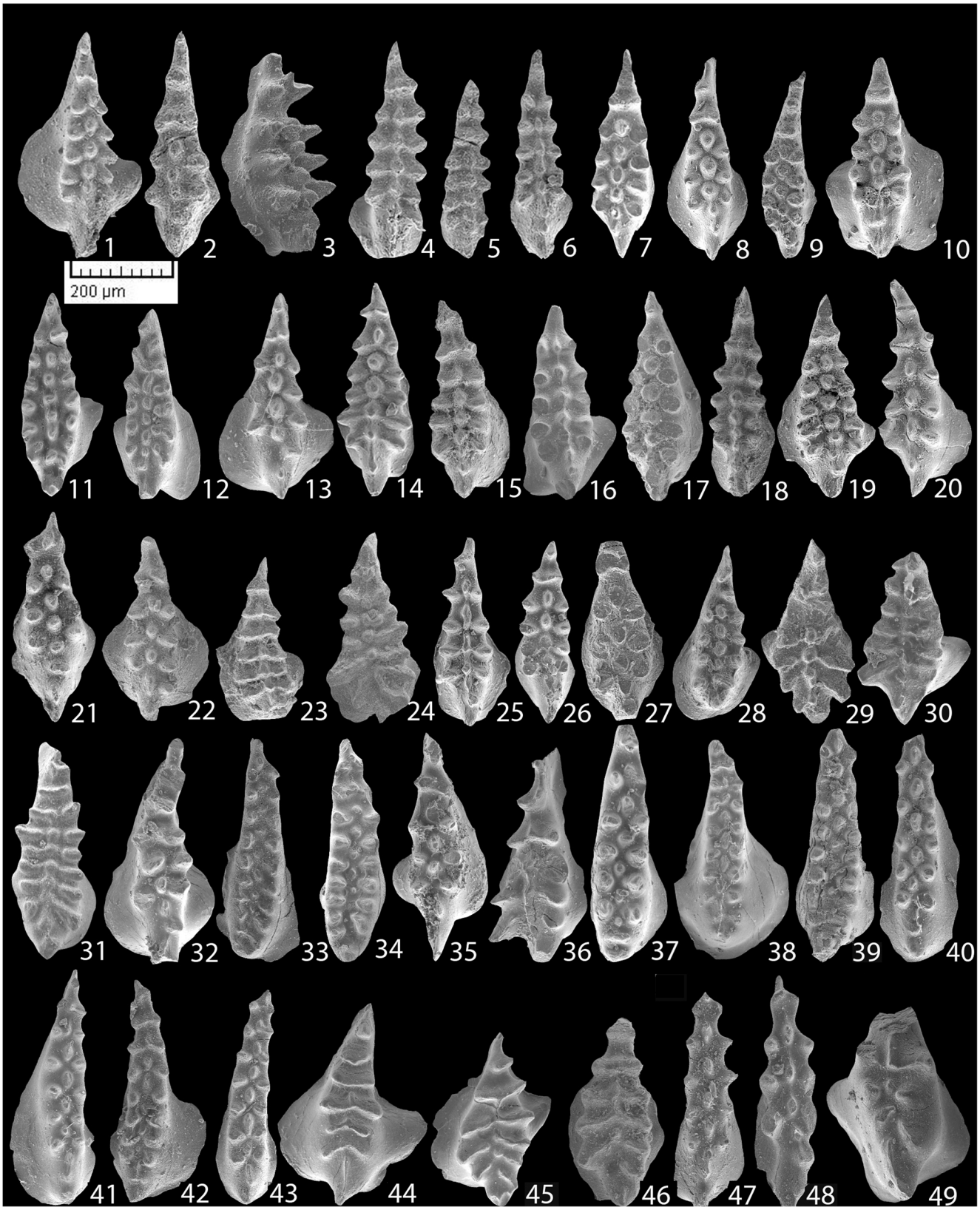

and *Bispathodus*. The overall specimen frequency is highly variable, ranging from a very low number of specimens (< 10 specimens per sample) to a good record (> 50 specimens per sample). The succession from "shallower" *Icriodus*-dominated samples to more "offshore" *Polygnathid*-dominated samples (e.g. Ziegler and Weddige 1999) are generally in agreement

◀**Fig. 6** **1**, **10–13** *Icriodus excavatus* Weddige, 1984; **1** upper view, Kuh-e-Bande-Abdol-Hossein (SE Anarak) section, northeast Isfahan, EUIC 224, sample S25, × 40; **10** upper view, Kuh-e-Bande-Abdol-Hossein (SE Anarak) section, northeast Isfahan, EUIC 239, sample S27, × 40; **11** upper view, Kuh-e-Bande-Abdol-Hossein (SE Anarak) section, northeast Isfahan, EUIC 242, sample S32, × 40; **12** upper view, Kuh-e-Bande-Abdol-Hossein (SE Anarak) section, northeast Isfahan, EUIC 243, sample S102, × 40; **13** upper view, Kuh-e-Bande-Abdol-Hossein (SE Anarak) section, northeast Isfahan, EUIC 268, sample S102, × 40. **2–3** *Icriodus brevis* Stauffer, 1940; **2** upper view, Kuh-e-Bande-Abdol-Hossein (SE Anarak) section, northeast Isfahan, EUIC 228, sample S25, × 40; **3** upper view, Kuh-e-Bande-Abdol-Hossein (SE Anarak) section, northeast Isfahan, EUIC 346, sample S32, × 40. **4–6** *Icriodus eslaensis* Adrichem Boogaert, 1967; **4** upper view, Kuh-e-Bande-Abdol-Hossein (SE Anarak) section, northeast Isfahan, EUIC 229, sample S21, × 40; **5** upper view, Kuh-e-Bande-Abdol-Hossein (SE Anarak) section, northeast Isfahan EUIC 230, sample S21, × 40; **6** upper view, Kuh-e-Bande-Abdol-Hossein (SE Anarak) section, northeast Isfahan EUIC 231, sample S25, × 40. **7–9** *Icriodus cedarensis* Narkiewicz and Bultynck, 2010; **7** upper view, Kuh-e-Bande-Abdol-Hossein (SE Anarak) section, northeast Isfahan, EUIC 233, sample S88, × 40; **8** upper view, Kuh-e-Bande-Abdol-Hossein (SE Anarak) section, northeast Isfahan, EUIC 236, sample S102, × 40; **9** upper view, Kuh-e-Bande-Abdol-Hossein (SE Anarak) section, northeast Isfahan, EUIC 237, sample S88, × 40. **14–18** *Icriodus expansus* Branson and Mehl, 1938; **14** upper view, Kuh-e-Bande-Abdol-Hossein (SE Anarak) section, northeast Isfahan, EUIC 244, sample S27, × 40; **15** upper view, Kuh-e-Bande-Abdol-Hossein (SE Anarak) section, northeast Isfahan, EUIC 247, sample S88, × 40; **16** upper view, Kuh-e-Bande-Abdol-Hossein (SE Anarak) section, northeast Isfahan, EUIC 365, sample S106, × 40; **17** upper view, Kuh-e-Bande-Abdol-Hossein (SE Anarak) section, northeast Isfahan, EUIC 367, sample S106, × 40; **18** upper view, Kuh-e-Bande-Abdol-Hossein (SE Anarak) section, northeast Isfahan, EUIC 374, sample S21, × 40. **19–22**, **36** *Icriodus subterminus* Youngquist, 1974; **19** upper view, Kuh-e-Bande-Abdol-Hossein (SE Anarak) section, northeast Isfahan, EUIC 249, sample S40, × 40; **20** upper view, Kuh-e-Bande-Abdol-Hossein (SE Anarak) section, northeast Isfahan, EUIC 255, sample S88, × 40; **21** upper view, Kuh-e-Bande-Abdol-Hossein (SE Anarak) section, northeast Isfahan, EUIC 257, sample S95, × 40; **22** upper view, Kuh-e-Bande-Abdol-Hossein (SE Anarak) section, northeast Isfahan, EUIC 361, sample S102, × 40; **36** upper view, Kuh-e-Bande-Abdol-Hossein (SE Anarak) section, northeast Isfahan, EUIC 289, sample S102, × 40. **23–24** *Icriodus norfordi* Chatterton, 1978; **23** upper view, Kuh-e-Bande-Abdol-Hossein (SE Anarak) section, northeast Isfahan, EUIC 260, sample S88, × 40; **24** upper view, Kuh-e-Bande-Abdol-Hossein (SE Anarak) section, northeast Isfahan, EUIC 368, sample S95, × 40. **25–26** *Icriodus latecarinatus* Bultynck, 1974; **25** upper view, Kuh-e-Bande-Abdol-Hossein (SE Anarak) section, northeast Isfahan, EUIC 261, sample S88, × 40; **26** upper view, Kuh-e-Bande-Abdol-Hossein (SE Anarak) section, northeast Isfahan, EUIC 262, sample S95, × 40. **27–29** *Icriodus lilliputensis* Bultynck, 1987; **27** upper view, Kuh-e-Bande-Abdol-Hossein (SE Anarak) section, northeast Isfahan, EUIC 265, sample S109 × 40; **28** upper view, Kuh-e-Bande-Abdol-Hossein (SE Anarak) section, northeast Isfahan, EUIC 266, sample S35 × 40; **29** upper view, Kuh-e-Bande-Abdol-Hossein (SE Anarak) section, northeast Isfahan, EUIC 379, sample S102, × 40. **30** *Icriodus arkonensis* Stauffer, 1938; upper view, Kuh-e-Bande-Abdol-Hossein (SE Anarak) section, northeast Isfahan, EUIC 271, sample S21, × 40. **31** *Icriodus difficilis* Ziegler, Klapper, 1976; upper view, Kuh-e-Bande-Abdol-Hossein (SE Anarak) section, northeast Isfahan, EUIC 272, sample S102, × 40. **32–34** *Icriodus praealternatus* Sandberg, Ziegler, Dreesen, 1992; **32** upper view, Kuh-e-Bande-Abdol-Hossein (SE Anarak) section, northeast Isfahan, EUIC 276, sample S233, × 40; **33** upper view, Kuh-e-Bande-Abdol-Hossein (SE Anarak) section, northeast Isfahan, EUIC 324, sample S262, × 40; **34** upper view, Kuh-e-Bande-Abdol-Hossein (SE Anarak) section, northeast Isfahan, EUIC 325, Sample S287, × 40. **35** *Icriodus cornutus* Sannemann, 1955; upper view, Kuh-e-Bande-Abdol-Hossein (SE Anarak) section, northeast Isfahan, EUIC 277, sample S310, × 40. **37–39** *Icriodus alternatus alternatus* Branson and Mehl, 1934; **37** upper view, Kuh-e-Bande-Abdol-Hossein (SE Anarak) section, northeast Isfahan, EUIC 281, sample S310, × 40; **38** upper view, Kuh-e-Bande-Abdol-Hossein (SE Anarak) section, northeast Isfahan, EUIC 306, sample S310, × 40; **39** upper view, Kuh-e-Bande-Abdol-Hossein (SE Anarak) section, northeast Isfahan, EUIC 314, sample S310, × 40. **40–43** *Icriodus alternatus helmsi* Sandberg and Dreesen, 1984; **40** upper view, Kuh-e-Bande-Abdol-Hossein (SE Anarak) section, northeast Isfahan, EUIC 299, sample S310, × 40; **41** upper view, Kuh-e-Bande-Abdol-Hossein (SE Anarak) section, northeast Isfahan, EUIC 301, sample S301, × 40; **42** upper view, Kuh-e-Bande-Abdol-Hossein (SE Anarak) section, northeast Isfahan, EUIC 304, sample S310, × 40; **43** upper view, Kuh-e-Bande-Abdol-Hossein (SE Anarak) section, northeast Isfahan, EUIC 288, sample S262, × 40. **44–46** *Icriodus iowaensis* Youngquist and Peterson, 1947; **44** upper view, Kuh-e-Bande-Abdol-Hossein (SE Anarak) section, northeast Isfahan, EUIC 290, sample S262, × 40; **45** upper view, Kuh-e-Bande-Abdol-Hossein (SE Anarak) section, northeast Isfahan, EUIC 329, sample S287, × 40; **46** upper view, Kuh-e-Bande-Abdol-Hossein (SE Anarak) section, northeast Isfahan, EUIC 327, sample S300, × 40. **47–48** *Icriodus symmetricus* Bransoan and Mehl, 1934; **47** upper view, Kuh-e-Bande-Abdol-Hossein (SE Anarak) section, northeast Isfahan, EUIC 328, sample S147, × 40; **48** upper view, Kuh-e-Bande-Abdol-Hossein (SE Anarak) section, northeast Isfahan, EUIC 383, sample S218, × 40. **49** *Icriodus deformatus asymmetricus* Ji, 1989; upper view, Kuh-e-Bande-Abdol-Hossein (SE Anarak) section, northeast Isfahan, EUIC 387, sample S310, × 40

with the sedimentological/facies record, but due to the limited conodont specimen per sample in some layers, the conodont biofacies provide generalised information and cannot be used to describe palaeoenvironmental settings in detail. Most of the analysed conodont taxa of the Kuh-e-Bande-Abdol-Hossein section are cosmopolitan.

The first conodont sample (sample S21) shows an *Icriodid-Polygnathid* biofacies with a small proportion of *Polygnathus linguiformis* (10%) at the base of the section. The occurrence of *Polygnathus linguiformis* is remarkable as the shallow-water/nearshore facies was obviously not a habitat of *P. linguiformis*. This species was adapted to more offshore, deeper water settings (Narkiewicz et al., 2016 and references therein). The next samples (S22 to S98), in the Givetian, are composed of 100% *Icriodus* species (Table 1, Fig. 8). Thus, the application of an alternative conodont zonation for this part of the section, proposed by Narkiewicz and Bultynck (2007, 2010), Bultynck and Gouwy (2008) and Narkiewicz (2011), was used. Among the icriodids, the most abundant species was *Icriodus expansus* Branson and Mehl, 1938 which may reach 70% of the conodont samples (Table 1, e.g. sample S26). The first appearance of *Ancyrodella* cf. *Ad. pristina* in the section corresponds with the first thin-bedded limestones just below greyish shales where we placed the Givetian/Frasnian boundary (Fig. 3). The changing lithology corresponds to a changing biofacies. Even if the total number of conodonts is low, polygnathids represent 26% of the assemblage whereas icriodid species reach 51%. From this interval, up to the Late Frasnian, conodont biofacies were generally dominated by polygnathid fauna which may represent more

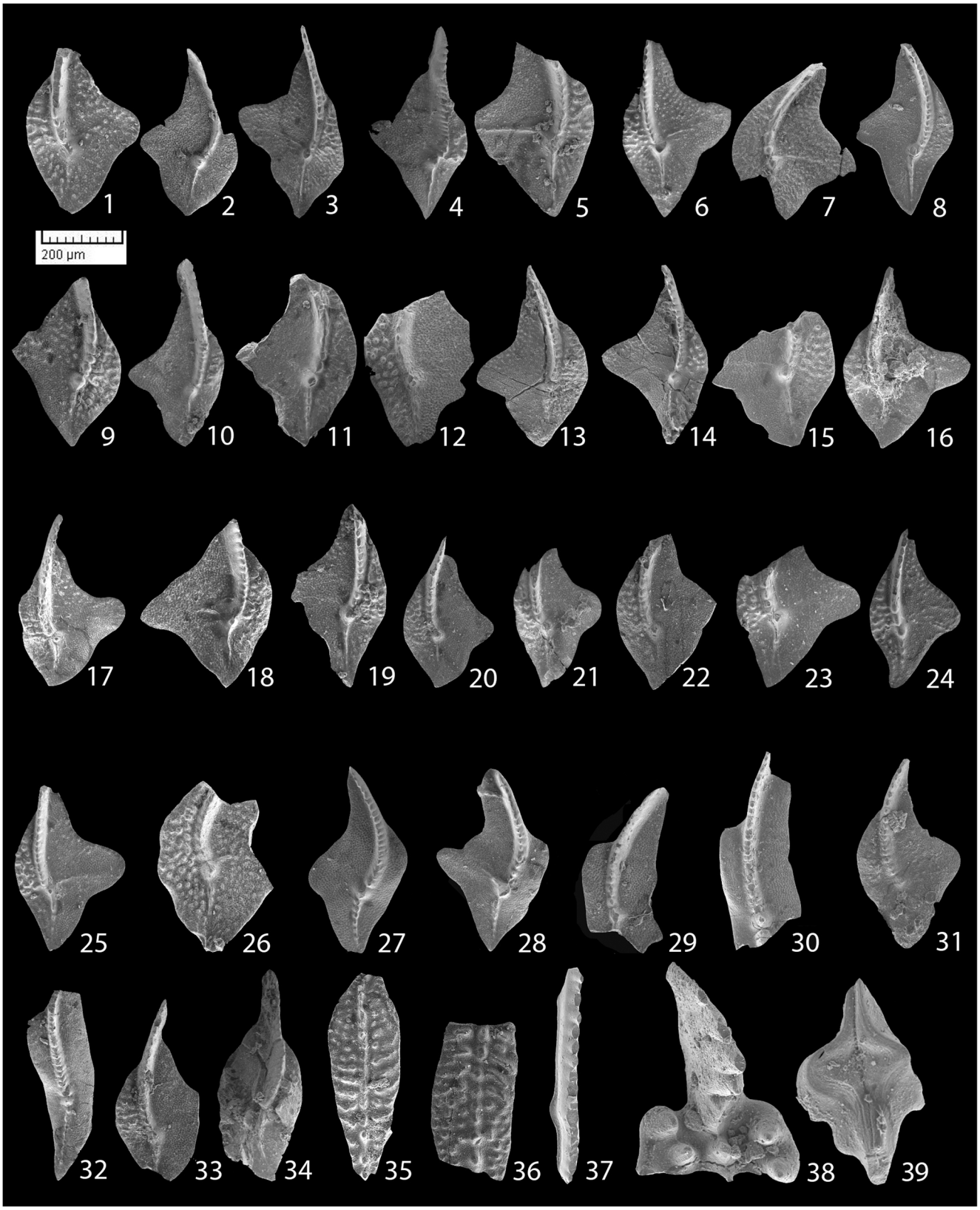

open marine conditions, which is corroborated by the lithology of the rocks. Among the polygnathids, *Po. webbi* and *Po. brevilaminus* reach their peak abundances in that part of the section. There is one remarkable interval (sample S150) within the upper *falsiovalis* to *transitans* zones where the conodont assemblage exhibit *Icriodus* species only. This abrupt change

◀**Fig. 7** **1–4**, **6** *Palmatolepis quadrantinodosalobata* Sannemann, 1955; **1** upper view, Kuh-e-Bande-Abdol-Hossein (SE Anarak) section, northeast Isfahan, EUIC 398, sample S310, × 40; **2** upper view, Kuh-e-Bande-Abdol-Hossein (SE Anarak) section, northeast Isfahan, EUIC 399, sample S310, × 40; **3** upper view, Kuh-e-Bande-Abdol-Hossein (SE Anarak) section, northeast Isfahan, EUIC 400, sample S310, × 40; **4** upper view, Kuh-e-Bande-Abdol-Hossein (SE Anarak) section, northeast Isfahan, EUIC 401, sample S310, × 40; **6** upper view, Kuh-e-Bande-Abdol-Hossein (SE Anarak) section, northeast Isfahan, EUIC 396, sample S310, × 40. **5**, **7**, **9**, **18** *Palmatolepis triangularis* Sannemann, 1955; **5** upper view, Kuh-e-Bande-Abdol-Hossein (SE Anarak) section, northeast Isfahan, EUIC 395, sample S310, × 40; **7** upper view, Kuh-e-Bande-Abdol-Hossein (SE Anarak) section, northeast Isfahan, EUIC 397, sample S310, × 40; **9** upper view, Kuh-e-Bande-Abdol-Hossein (SE Anarak) section, northeast Isfahan, EUIC 409, sample S310, × 40; **18** upper view, Kuh-e-Bande-Abdol-Hossein (SE Anarak) section, northeast Isfahan, EUIC 391, sample S310, × 40. **8**, **27**, **28** *Palamtolepis* aff. *tenuipunctata* Sannemann, 1955; **8** upper view, Kuh-e-Bande-Abdol-Hossein (SE Anarak) section, northeast Isfahan, EUIC 418, sample S310, × 40; **27** upper view, Kuh-e-Bande-Abdol-Hossein (SE Anarak) section, northeast Isfahan, EUIC 411, sample S310, × 40; **28** upper view, Kuh-e-Bande-Abdol-Hossein (SE Anarak) section, northeast Isfahan, EUIC 407, sample S310, × 40. **10**, **16**, **17**, **31** *Palmatolepis quadrantinodosalobata* Sannemann, 1955 morphotype 1; **10** upper view, Kuh-e-Bande-Abdol-Hossein (SE Anarak) section, northeast Isfahan, EUIC 404, sample S310, × 40; **16** upper view, Kuh-e-Bande-Abdol-Hossein (SE Anarak) section, northeast Isfahan, EUIC 422, sample S310, × 40; **17** upper view, Kuh-e-Bande-Abdol-Hossein (SE Anarak) section, northeast Isfahan, EUIC 423, sample S310, × 40; **18** upper view, Kuh-e-Bande-Abdol-Hossein (SE Anarak) section, northeast Isfahan, EUIC 424, sample S310, × 40; **31** upper view, Kuh-e-Bande-Abdol-Hossein (SE Anarak) section, northeast Isfahan, EUIC 419, sample S310, × 40. **13–14**, **19** *Palmatolepis sandbergi* Ji and Ziegler, 1993 morphotype 1; **13** upper view, Kuh-e-Bande-Abdol-Hossein (SE Anarak) section, northeast Isfahan, EUIC 416, sample S310, × 40; **14** upper view, Kuh-e-Bande-Abdol-Hossein (SE Anarak) section, northeast Isfahan, EUIC 417, sample S310, × 40; **19** upper view,, Kuh-e-Bande-Abdol-Hossein (SE Anarak) section, northeast Isfahan, EUIC 388, sample S310, × 40; **20–25** *Palmatolepis quadrantinodosalobata* Sannemann, 1955 morphotype 3; **20** upper view, Kuh-e-Bande-Abdol-Hossein (SE Anarak) section, northeast Isfahan, EUIC 392, sample S310, × 40; **21** upper view, Kuh-e-Bande-Abdol-Hossein (SE Anarak) section, northeast Isfahan, EUIC 389, sample S310, × 40; **22** upper view, Kuh-e-Bande-Abdol-Hossein (SE Anarak) section, northeast Isfahan, EUIC 394, sample S310, × 40; **23** upper view, Kuh-e-Bande-Abdol-Hossein (SE Anarak) section, northeast Isfahan, EUIC 394, sample S310, × 40; **24** upper view, Kuh-e-Bande-Abdol-Hossein (SE Anarak) section, northeast Isfahan, EUIC 390, sample S310, × 40; **25** upper view, Kuh-e-Bande-Abdol-Hossein (SE Anarak) section, northeast Isfahan, EUIC 390, sample S310, × 40. **11**, **12**, **15**, **26** *Palmatolepis* aff. *quadrantinodosalobata* Sannemann, 1955 morphotype 1; **11** upper view, Kuh-e-Bande-Abdol-Hossein (SE Anarak) section, northeast Isfahan, EUIC 405, sample S310, × 40; **12** upper view, Kuh-e-Bande-Abdol-Hossein (SE Anarak) section, northeast Isfahan, EUIC 406, sample S310, × 40; **15** upper view, Kuh-e-Bande-Abdol-Hossein (SE Anarak) section, northeast Isfahan, EUIC 420, sample S310, × 40; **26** upper view, Kuh-e-Bande-Abdol-Hossein (SE Anarak) section, northeast Isfahan, EUIC 410, sample S310, × 40. **29**, **30**, **32** *Palamtolepis glabra pectinata* Ziegler, Ji and Ziegler, 1993 1962; **29** upper view, Kuh-e-Bande-Abdol-Hossein (SE Anarak) section, northeast Isfahan, EUIC 408, sample S310, × 4; **30** upper view, Kuh-e-Bande-Abdol-Hossein (SE Anarak) section, northeast Isfahan, EUIC 403, sample S310, × 40; **32** upper view, Kuh-e-Bande-Abdol-Hossein (SE Anarak) section, northeast Isfahan, EUIC 421 sample S300, × 40. **33** *Palamtolepis* cf. *delicatula* Branson and Mehl, 1034; upper view, Kuh-e-Bande-Abdol-Hossein (SE Anarak) section, northeast Isfahan, EUIC 412, sample S310, × 40. **34** *Palmatolepis* cf. *termini* Sannemann, 1955; upper view, Kuh-e-Bande-Abdol-Hossein (SE Anarak) section, northeast Isfahan, EUIC 183, sample S310, × 40. **35**, **36** *Ancyrognathus sinelaminus* Branson and Mehl, 1934; **35** upper view, Kuh-e-Bande-Abdol-Hossein (SE Anarak) section, northeast Isfahan, EUIC 186, sample S310, × 40; **36** upper view, Kuh-e-Bande-Abdol-Hossein (SE Anarak) section, northeast Isfahan, EUIC 184, sample S310, × 40. **37** *Bispathodus stabilis* Branson and Mehl, 1934, morphotype 1; upper view, Kuh-e-Bande-Abdol-Hossein (SE Anarak) section, northeast Isfahan, EUIC 184, sample S310, × 40. **38–39** *Ancyrodella* cf. *pristina* Khalymbadzha and Chernysheva, 1970; **38** upper view, Kuh-e-Bande-Abdol-Hossein (SE Anarak) section, northeast Isfahan, EUIC 425, sample S102, × 40; **39** upper view, Kuh-e-Bande-Abdol-Hossein (SE Anarak) section, northeast Isfahan, EUIC 292, sample S102, × 40

in biofacies is most probably linked with local features and it is hard to correlate this interval with known events such as the Timan Event which occurs in the *transitans* Zone. Furthermore, the latter one is linked with a transgressive phase and faunal blooms (Becker et al. 2016) rather than shallowing. The overlying interval of the *transitans* to Lower *rhenana* zones (Fig. 8) generally exhibit assemblages which belong to the *Polygnathid-Icriodid* biofacies which are dominated by polygnathids. The disadvantage in that part of the section is the lack of a high-resolution biostratigraphical framework as a result of hiatuses. The next younger unit of the Upper *rhenana* to *linguiformis* zones exhibit two shallow-water intervals with an increase in icriodid species. Icriodid species represent 100% of sample S249. *Icriodus iowaensis* Youngquist and Peterson, 1947 is very abundant (> 50 specimens) which occurs together with *Icriodus alternatus helmsi* Sandberg and Dreesen, 1984. This interval is overlain by thin-bedded limestones which yield only polygnathids, but the number of species is very low. The upper part of the Frasnian exhibits an increasing number of icriodid species and polygnathids are less common. The changing biofacies record in the Upper *rhenana* to *linguiformis* zones point to sea level changes which correspond to lithological change. Based on the limited biostratigraphic control, it is questionable whether the deepening in the Upper *rhenana* to *linguiformis* zones correspond to the proposed eustatic rise by Sandberg et al. (2002) ranging from the Upper *rhenana* Zone into the *linguiformis* Zone or if this sea level change was triggered by local tectonics. First sedimentological/facies interpretation support this assumption, but more detailed work is necessary. In the upper part of the Frasnian, which may correspond to the *linguiformis* Zone, *Icriodus alternatus* is abundant (samples S262–S300, up to 36%), whereas this species had been a minor constituent of conodont faunas below. This may support shallowing in the *linguiformis* Zone. Similar changes in shallow-water conodont fauna were reported by Sandberg et al. (2002). Conodont biofacies are characterised by *Polygnathid-Icriodid* biofacies with accessory components of *Palmatolepis* and *Ancyrodella.* The youngest part of the section represents Famennian deposits with *Ancyrognathus* and *Bispathodus*.

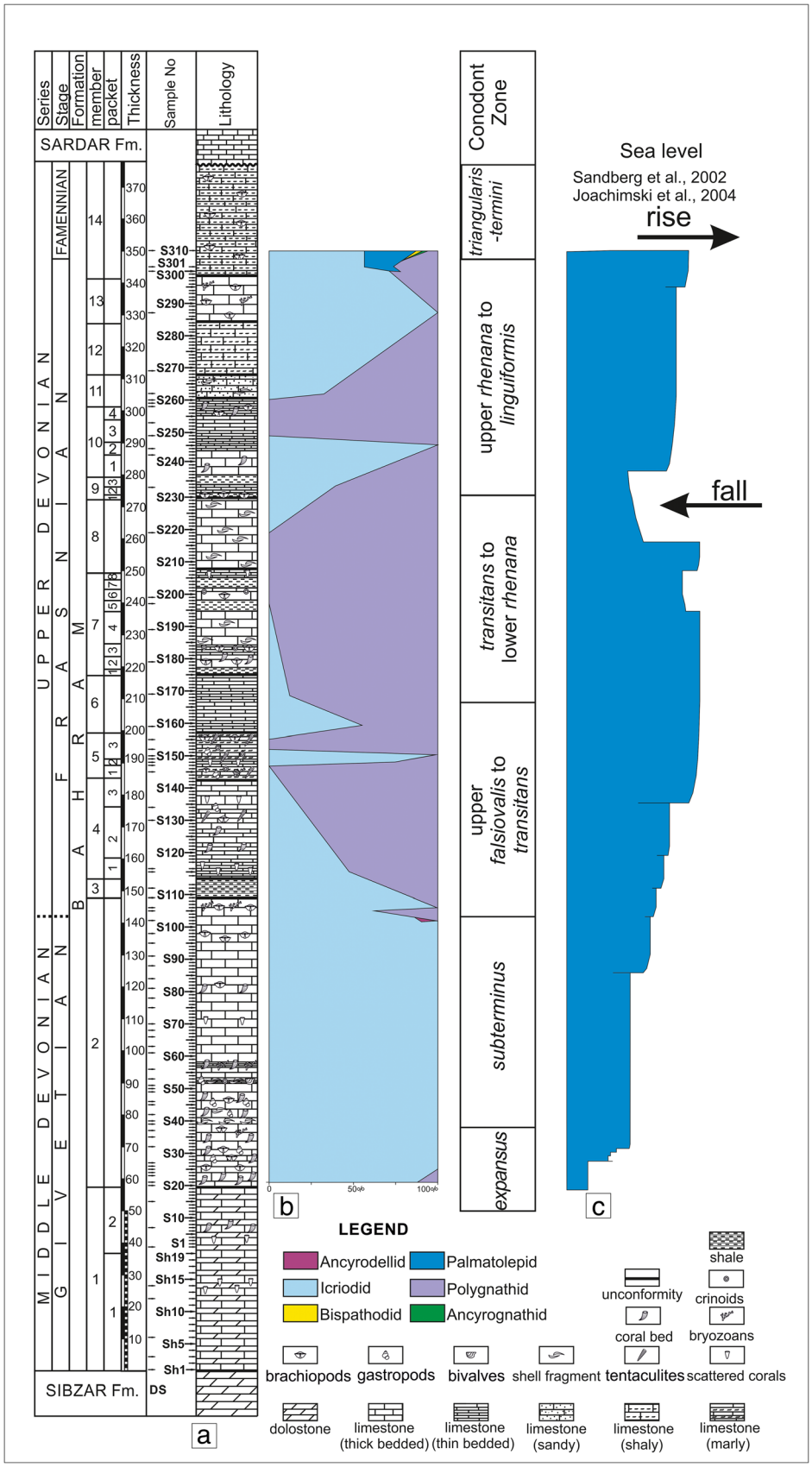

Fig. 8 Conodont biofacies of the studied section. **a** Stratigraphic column. **b** Conodont biofacies. **c** Sea level changes according to Sandberg et al. (2002) and Joachimski et al. (2004)

Table 1 Conodont element distribution and number of elements of the Kuh-e-Bande-Abdol-Hossein section

Kuh-e-Bande-Abdol-Hossein - Anarak	S21	S25	S27	S32	S35	S40	S51	S56	S63	S81	S82	S88	S95	S98	S102	S105	S109	S115	S147	S149	S150	S152	S155	S159	S169	S197	S199	S219	S233	S242	S249	S260	S262	S287	S300	S301	S310	TOTAL
Ancyrodella cf. *pristina*																2																							2
Ancyrognathus sinelaminus																																					2	2
Bispathodus stabilis																																					3	3
Icriodus alternatus helmsi																														2			7	4	3	1	9	26
Icriodus alt. alternatus																													2				18	6	17	34	46	123
Icriodus iowaenssis																														56			6	6	3			71
Icriodus praealternatus																													2				3	1				6
Icriodus brevis	23	4	5	34											23																							89
Icriodus cedarensis												5			6						3																	14
Icriodus liliputensis					9							16			5	6	8	2																				46
Icriodus latecarinatus												7	5																									12
Icriodus subterminus						4	6	8	7			4	9	2																									40
Icriodus cornutus																																					9	9
Icriodus difficilis										1	4	9			5																							19
Icriodus eslaensis	2	9																																				11
Icriodus expansus	9		67		54							23			13	2					8																	176
Icriodus excavatus		5	3	2								2		5																									17
Icriodus arkonensis	8																																					8
Icriodus deformatus asymmetricus																																					4	4
Palmatolepis glabra pectinata																																					5	5
Palmatolepis cf. *delicatula*																																					1	1
Palmatolepis cf. *termini*																																					1	1
Palmatolepis triangularis																																					9	9
Palmatolepis quadrantinodosalobata																																					6	6
Palmatolepis sandbergi																																					3	3
Palmatolepis tenuipunctata																																					7	7
Polygnathus evidens																									1		2	1							4			8
Polygnathus brevilaminus																											65					54	43			5		167
Polygnathus aequalis																									7		9						11					27
Polygnathus alatus													1			2		3		4		1		5	6						4	2	5		1	1		35
Polygnathus krestovnikovi																													2				1	1	1	1		6
Polygnathus angustidiscus																											3	2										5
Polygnathus granulosa																																					6	6
Polygnathus nodocostatus																																					6	6
Polygnathus zinaidae																									9		6	12										27
Polygnathus cf. *semicostatus*																																					8	8
Polygnathus ling. linguifromis γ 1a	5																																					5
Polygnathus pseudoxylus																									15		12	3										30
Polygnathus politus																											24	8	3		9		8		4	5		61
Polygnathus webbi																			65			13	35		7		1	1			8	9	7		1	1		148
Polygnathus xylus												2			6	6		12							2													20
unassigned elements	2	8	12	1	5	3	15	1	1	4	1	9	14	5	6	7	123	12	18	69	3	17	12	13	89	12	53	1	13	14	16	12	13	15	9	9	1	648
TOTAL	49	26	87	37	80	7	21	9	8	5	5	77	28	7	59	31	150	53	83	73	19	31	84	24	143	77	99	11	16	72	37	87	122	31	40	81	131	1917

Concluding remarks

The Kuh-e-Bande-Abdol-Hossein section is composed of an overall shallow-water, nearshore to open marine facies setting. A detailed biostratigraphic record based on conodonts is difficult due to the facies setting, many conodont samples lack relevant zonal index taxa and secondly, the entire section—as other Middle to Late Devonian sections in Central Iran—exhibit remarkable hiatuses in the sedimentological record which is most likely a result of synsedimentary tectonics (horst and graben structures).

Apart from well-defined stratigraphy, it is difficult to precisely pinpoint equivalents of global event layers which may occur even if lithological evidence is lacking. The Kuh-e-Bande-Abdol-Hossein section provides evidence of one event at the Givetian/Frasnian boundary. This is based on the conodont biostratigraphy, the changing lithology and conodont biofacies. A proposed rapid sea level rise can be correlated with the Frasne-Event. Further evidence that this transgression is not a local feature is supported by detailed studies of the Zefreh section (Königshof et al. 2017) which is located approximately 250 km to the west. We conclude that this transgression is linked with a major sequence boundary recorded in the Cedar Valley Group in Iowa, USA (Johnson et al. 1985; Witzke et al. 1996; Brett et al. 2011).

The biofacies concept provides some palaeoecological information and generally confirms lithological changes in the sediments, but should be applied with caution in shallow-water palaeoenvironments due to abrupt lateral facies changes, limited conodont record and hiatuses. Thus, a more detailed sedimentologic/facies record is necessary in order to establish a detailed facies interpretation.

Conodonts found in the last 10 m of the section exhibit a very wide stratigraphical range, from the *termini* to *Palmatolepis* gr. *expansus* zones which support the assumption by Wendt et al. (2005) that there is a major gap in Central Iran (including reworked material) which comprises large parts of the Famennian.

Acknowledgements We thank both reviewers Thomas Suttner (Vienna, Austria) and Jeff Over (Geneseo, NY, USA) for their constructive comments.

Funding information The authors thank the University of Isfahan, IR Iran, for financial and logistic support. Funding by the second author (P.K.) is acknowledged by the Deutsche Forschungsgemeinschaft (DFG Project KO-1622/16-1).

Compliance with ethical standards

Conflict of interest The author declares that he has no conflict of interest.

References

Adrichem Boogaert, H. A. (1967). Devonian and lower Carboniferous conodonts of the Cantabrian Mountains (Spain) and their stratigraphic application. *Geologische Mededelingen, 39*, 129–192.

Aghanabati, A. (2010). Stratigraphy of Iran. Geological Survey of Iran, Tehran, 1297 p.

Almasian, M (1997). Tectonics of the Anarak area (Central Iran). Ph.D. thesis, *University of Islamic Azad, Science and Research Unit*, 164 p.

Bahrami, A., Boncheva, I., Königshof, P., Yazdi, M., & Ebrahimi Khan-Abadi, A. (2014a). Mississippian/Pennsylvanian boundary interval in Central Iran. *Journal of Asian Earth Sciences, 92*, 187–200. https://doi.org/10.1016/j.jseaes.2014.06.017.

Bahrami, A., Königshof, P., Boncheva, I., Tabatabaei, M. S., Yazdi, M., & Safari, Z. (2015). Middle Devonian (Givetian) conodonts from the northern margin of Gondwana (Soh and Natanz regions, north-west Isfahan, Central Iran): biostratigraphy and palaeoenvironmental implications. *Palaeobiodiversity and Palaeoenvironments, 95*(4), 555–577. https://doi.org/10.1007/s12549-015-0205-0.

Bahrami, A., Königshof, P., Boncheva, I., Yazdi, M., Ahmadi Nahre Khalaji, M., & Zarei, E. (2018). Conodont biostratigraphy of the Kesheh and Dizlu sections, and the age range of the Bahram Formation in Central Iran. *Palaeobiodiversity and Palaeoenvironments, 98*, 315–329. https://doi.org/10.1007/s12549-017-0307-y.

Bahrami, A., Zamani, F., Corradini, C., Yazdi, M., & Ameri, H. (2014b). Late Devonian (Frasnian) conodonts from the Bahram Formation, in the Sar-e- Ashk section, Kerman province, Central-East Iran Microplate. *Bollettino della Società Paleontologica Italiana., 53*(3), 179–188.

Becker, R.T., Königshof, P., & Brett, C.E. (Eds). (2016). Devonian climate, sea level and evolutionary events: An introduction. *Geological Society of London, Special Publication, 432*, 1–10. https://doi.org/10.1144/SP423.15.

Berberian, M., & King, G. C. P. (1981). Towards a paleogeography and tectonic evolution of Iran. *Canadian Journal of Earth Sciences, 18*, 210–265.

Bischoff, G., & Ziegler, W. (1957). Die Conodontenchronologie des Mitteldevons und des tiefsten Oberdevons. *Abhandlungen des Hessischen Landesamtes für Bodenforschung, 22*, 1–136

Branson, E. B., & Mehl, M. G. (1934). Conodonts from the grassy creek shale of Missouri. *The University of Missouri Studies, 8*, 171–259

Brett, C. E., Baird, G. C., Bartholomew, A. J., DeSantis, M. K., & Ver Straaten, C. A. (2011). Sequence stratigraphy and a revised sea-level curve for the Middle Devonian of eastern North America. In C. E. Brett, E. Schindler, & P. Königshof, (Eds.) Sea-level cyclicity, climate change, and bioevents in Middle Devonian marine and terrestrial environments. *Palaeogeography, Palaeoclimatology, Palaeoecology, 304*(1–2), 21–53.

Bultynck, P. (1974). Conodontes de la Formation de Fromelennes du Givetien del'Ardenne franco-belge. *Bulletin de l'Institut Royal des Sciences Naturelles de Belgique. Sciences de la Terre, 50*, 1–30.

Bultynck, P. (1987). Pelagic and neritic conodont successions from the Givetian of pre-Sahara Morocco and the Ardennes. *Bulletin van het Koninklijk Belgisch Instituut voor Natuurwetenschappen, Aardwetenschappen, 57*, 149–181.

Bultynck, P., & Gouwy, S. (2008). Reference sections for the Middle Givetian substage. *Subcommission on Devonian Stratigraphy Newsletter, 23*, 21–26.

Chatterton, B. D. E. (1978). Aspects of late Early and Middle Devonian conodont biostratigraphy of western and northwestern Canada. Western and Arctic Canadian biostratigraphy. Edited by C.R., Stelck, and Chatteron, B.D.E., *Geological Association of Canada. Special Paper, 18*, 161–231.

Clausen, C. D., Weddige, K., & Ziegler, W. (1993). Devonian of the Rhenish Massif. *Subcommission on Devonian Stratigraphy, Newsletter, 10*, 18–19.

Corradini, C. (1998). Famennian conodonts from two sections near Vilasalto. In E. Serpagli (Ed.) Seventh International Conodont Symposium held in Europe, Sardegna Field Trip Guidebook, June 18-22, 1998. *Giornale die Geologica*, *Serie 3a*, Special Issue, 60, 122–135.

Flügel, E., & Kiessling, W. (2002). Patterns of Phanerozoic reef crises. In W. Kiessling, E. Flügel, & J. Golonka (Eds.) *Phanerozoic reef Patterns SEPM Special Publication,* 72, 691–733.

Ernst, A., Königshof, P., Bahrami, A., Yazdi, M., & Boncheva, I. (2017). A Late Devonian (Frasnian) bryozoan fauna from the central Iran. In B. Mottequin, L. Slavik & P. Königshof (Eds.) *Climate change and biodiversity patterns in the mid-Palaeozoic. Palaeobiodiversity and Palaeoenvironments, 97*(3), 541–552. https://doi.org/10.1007/s12549-016-0269-5.

Hairapetian, V., Ghobadi Pour, M., Popov, L. E., Hejazi, S. H., & Holmer, L. E. (2015). Ordovician of the Anarak region: implications in understanding Early Palaeozoic history of Central Iran. *Stratigraphy, 12*(2), 22–30.

Hinde, G. J. (1879). On conodonts from the Chazy and Cincinnati group of the Cambro-Silurian and from the Hamilton and Genesee shale divisions of the Devonian in Canada and the United States. *Geological Society of London Quarterly Journal, 35*(3), 351–369.

Houshmandzadeh, A. (1977). Metamorphism et granitisation du massif Chapedony (Iran Central). – 242 pp; Thesis (Universitè Scientifique et Medicale de Grenoble, France).

Huddle, J. W. (1934). Conodonts from the New Albany Shale of Indiana. *Bulletin America Paleontology, 21*, 1–136.

Ji, Q. (1989). On the Frasnian conodont biostratigraphy in the Guilin area of Guangxi, South China. *Courier Forschungsinstitut Senckenberg, 117*, 303–322.

Ji, Q., & Ziegler, W. (1993). The Lali section: an excellent reference section for Late Devonian in South China. *Courier Forschungsinstitut Senckenberg, 157*, 183 p.

Joachimski, M. M., Breisig, S., Buggisch, W., Mawson, R., Gereke, M., Morrow, J. R., Day, J., & Weddige, K. (2009). Devonian climate and reef evolution: insights from oxygen isotopes in apatite. *Earth and Planet Science Letters, 284*, 599–609.

Johnson, J. G., Klapper, G., & Sandberg, C. A. (1985). Devonian eustatic fluctuations in Euramerica. *Geological Society of America Bulletin, 69*, 567–587.

Khalymbadzha, V. G., & Chernysheva, N. G. (1970). Conodont genus *Ancyrodella* from Devonian deposits of the Volga-Kamsky area and their stratigraphic significance: biostratigraphy and paleontology of Paleozoic deposits of the eastern Russian platform and western pre-Urals (in Russian). *Kazan University, 1*, 81–103.

Klapper, G., & Lane, H. R. (1985). Upper Devonian (Frasnian) conodonts of the Polygnathus biofacies, N.W.T., Canada. *Journal of Paleontology, 59*, 904–951.

Klapper, G., & Ziegler, W. (1979). Devonian conodont biostratigraphy. *Special Paper on Palaeontology, 23*, 199–224.

Kononova, L. I., Alekseev, A. S., Barskov, I. S., & Reimers, A. N. (1996). New species of polygnatoid conodonts from Frasnian of Moskow syneclise. *Paleontologicheskii Journal, 3*, 94–99.

Königshof, P., Da Silva, A. C., Suttner, T. J., Kido, E., Waters, J., Carmichael, S. K., Jansen, U., Pas, D., & Spassov, S. (2016). Shallow water facies setting around the Kacak Event—a multidisziplinary approach. In Becker, R.T., Königshof, P., & Brett C.E. (Eds.) Devonian climate, sea level and evolutionary events. *Geological Society London, Special Publication, 423*, 171–199. https://doi.org/10.1144/SP423.4.

Königshof, P., Carmichael, S. K., Waters, J., Jansen, U., Bahrami, A., Boncheva, I., & Yazdi, M. (2017). Palaeoenvironmental study of the Palaeotethys Ocean: the Givetian-Frasnian boundary of a shallow-marine environment using combined facies analysis and geochemistry (Zefreh Section/Central Iran). In B. Mottequin, L. Slavik, & P. Königshof (Eds.). *Climate change and biodiversity patterns in the mid-Paleozoic. Palaeobiodiversity and Palaeoenvironments, 97*(3), 517–540. https://doi.org/10.1007/s12549-016-0253-0 .

Lensch, G., & Davoudzadeh, M. (1982). Ophiolites in Iran. *Neues Jahrbuch für Geologie und Paläontologie Monatshefte*, 306–320.

Leven, E. J., & Gorgij, M. N. (2006). Upper Carboniferous Permian stratigraphy and Fusulinids from the Anarak region, Central Iran. *Russian Journal of Earth Sciences, 8*, 25.

Lüddecke, F., Hartenfels, S., & Becker, R. T. (2017). Conodont biofacies of a monotonous middle Famennian pelagic carbonate succession (Ballberg Quarry, northern Rhenish Massif). In B. Mottequin, L. Slavik & P. Königshof (Eds.) *Climate change and biodiversity patterns in the mid-Paleozoic. Palaeobiodiversity and Palaeoenvironments, 97*(3), 591–614.

Motaghi, K., Tatar, M., Priestley, K., Romanelli, F., Doglioni, C., & Panza, G. F. (2015). The deep structure of the Iranian Plateau. *Gondwana Research, 28*(1), 407–418.

Mottequin, L., Slavik, L. & Königshof, P. (2017). Increasing knowledge on biodiversity patterns and climate changes in Earth's history by international cooperation: introduction to the prceedings IGCP 596/SDS Meeting Brussels (2015). In B. Mottequin, L. Slavik & P. Königshof (Eds.) *Climate change and biodiversity patterns in the mid-Paleozoic. Palaeobiodiversity and Palaeoenvironments, 97*(3), 367–374.

Müller, K. J., & Muller, E. M. (1957). Early Upper Devonian (independence) conodonts from Iowa, part I. *Journal of Paleontology, 31*, 1069–1108.

Narkiewicz, K. (2011). Biostratygrafia konodontowa Dewonu Środkowego obszaru Radomsko-Lubelskiego. *Prace Panstwowego Instytutu Geologicznego, 196*, 147–192.

Narkiewicz, K., & Bultynck, P. (2007). Conodont biostratigraphy of shallow marine Givetian deposits from the Radom-Lublin area, SE Poland. *Geological Quarterly, 51*, 419–442.

Narkiewicz, K., & Bultynck, P. (2010). The Upper Givetian (Middle Devonian) subterminus conodont zone in North America, Europe, and North Africa. *Journal of Paleontology, 84*(4), 588–625.

Ovanatanova, N.S. (1969). New Upper Devonian conodonts from the central region of the Russian platform and of the Timan: In *Fauna and stratigraphy of the Palaeozoic of the Russian platform*. Nedra, 39–141.

Reyer, D., & Mohafez, S. (1970). Une premiere contribution des accords NIOC–ERAP a la connaissance geologique de l′ Iran. *Review Institute de France Petrology, 25*, 979–1014.

Sandberg, C. A. (1976). Conodont biofacies of Late Devonian polygnathus styriacus zone in western United State. In C.R. Barnes (Ed.). Conodont Paleoecoloy. *Geological Association of Canada*, Special Paper, 15, 171–186.

Sandberg, C.A. & Ziegler, W. (1979). Taxonomy and biofacies of important conodonts of Late Devonian styriacus-Zone, United States and Germany. *Geologica et Palaeontologica, 13*, 173–212.

Sandberg, C. A., & Dreesen, R. (1984). Late Devonian icriodontid biofacies models and alternate shallow water conodont zonation. In D. L. Clark (Ed.) Conodont biofacies and provincialism. *Geological Society of America,* Special Paper, *196*, 143–178.

Sandberg, C.A., Ziegler, W. & Bultynck, P. (1989). New standard conodont zones and early Ancyrodella phylogeny across Middle–Upper

Devonian boundary. *Courier Forschungsinstitut Senckenberg, 110*, 195–230.

Sandberg, C. A., Morrow, J. R., & Ziegler, W. (2002). Late Devonian sea-level changes, catastrophic events, and mass extinctions. In Koeberl, C. & MacLeod, K. G., (Eds.) Catastrophic events and mass extinctions: impacts and beyond: Boulder, Colorado, *Geological Society of America Special Paper*, *356*, 473–487.

Sannemann, D. (1955). Oberdevonische Conodonten (to IIa). *Senckenbergiana lethaea, 26*, 123–156.

Scotese, C. R. (2001). *Atlas of Earth-History. Paleogeography, Vol. 1*. Arlington, Texas. Paleomap Project.

Sharkovski, M., Susov, M., & Krivyakin, M. (1984). Geology of the Anarak area (Central Iran), explanatory text of the Anarak quadrangle map. *Geological Survey of Iran*, *Scale*, 1: 250. 000, V/O Technoexport, Report, 19. Tehran, 143 p.

Soffel, H. C., & Förster, H. G. (1984). Polar wander path of the Central-East-Iran Microplate including new results. *Neues Jahrbuch für Geologie und Paläontologie, Abhandlungen, 168*(2/3), 165–172.

Soffel, H. C., Davoudzadeh, M., Rolf, C., & Schmidt, S. (1996). New palaeomagnetic data from Central Iran and a Triassic palaeoreconstruction. *Geologische Rundschau, 85*, 293–302.

Söte, T., Hartenfels, S., & Becker, R. T. (2017). Uppermost Famennian stratigraphy and facies development of the Reigern Quarry near Hachen (northern Rhenish Massif, Germany). In B. Mottequin, L. Slavik & P. Königshof (Eds.) *Climate change and biodiversity patterns in the mid-Paleozoic*. *Palaeobiodiversity and Palaeoenvironments, 97*(3), 633–654.

Stauffer, C. R. (1938). Conodonts of the Olentangy Shale. *Journal of Paleontology, 12*, 411–433.

Stauffer, C. R. (1940). Conodonts from the Devonian and associated clays of Minnesota. *Journal of Paleontology, 14*(2), 417–435.

Weddige, K. (1984). Zur Stratigraphie und Paläogeographie des Devons und Karbons von NE Iran. *Senckenbergiana lethaea, 65*, 179–223.

Weddige, K., & Ziegler, W. (1979). The significance of *Icriodus*: *Polygnathus* ratios in limestones from the type Eifelian, Germany. *Geological Association of Canada Special Paper, 15*, 187–199.

Wendt, J., Hayer, J., & Karimi Bavandpour, A. (1997). Stratigraphy and depositional environment of Devonian sediments in northeast and east-Central Iran. *Neues Jahrbuch für Geologie und Paläontologie, Abhandlungen, 206*, 277–322.

Wendt, J., Kaufmann, B., Belka, Z., Farsan, N., & Karimi Bavandpur, A. (2002). Devonian/Lower Carboniferous stratigraphy, facies patterns and palaeogeography of Iran. Part I. Southeastern Iran. *Acta Geologica Polonica, 52*, 129–168.

Wendt, J., Kaufmann, B., Belka, Z., Farsan, N., & Karimi Bavandpur, A. (2005). Devonian/Lower Carboniferous stratigraphy, facies patterns and palaeogeography of Iran. Part II. Northern and Central Iran. *Acta Geologica Polonica, 55*, 31–97.

Witzke, B. J., Ludvigson, G. V., & Day, J. (1996). Introduction: Paleozoic applications of sequence stratigraphy. *Geological Society of America Special Papers, 1996*(306), 1–6.

Youngquist, W. L. (1947). A new Upper Devonian conodont fauna from Iowa. *Journal of Paleontology, 21*(2), 95–112.

Youngquist, W. L., & Peterson, R. F. (1947). Conodonts from the Sheffield Formation of north-Central Iowa. *Journal of Paleontology, 21*, 242–253.

Zahedi, M. (1973). Etude geologique de La region de Soh (W de Iran central). *Geological Survey of Iran*, *27*, 197, Tehran.

Ziegler, W., & Klapper, G. (1976). Systematic paleontology. In W., Ziegler, G., Klapper, & J. G., Johnson, (Eds.), Redefinition and subdivision of the varcus-zone (conodonts, Middle-? Upper Devonian) in Europe and North America. *Geologica et Palaeontologica, 10*, 117–127.

Ziegler, W., & Sandberg, C.A. (1984). Palmatolepis-based revision of upper part of standard Late Devonian conodont zonation. In Clark, D.L. (Ed.) Conodont biofacies and provincialism. *Geological Society of America Special Paper*, 179–194.

Ziegler, W., & Sandberg, C. A. (1990). The Late Devonian standard conodont zonation. *Courier Forschungsinstitut Senckenberg, 121*, 1–115.

Ziegler, W., & Sandberg, C. A. (1996). Reflexions on the Frasnian and Famennian stage boundary decisions as a guide to future deliberations. *Newsletters on Stratigraphy, 33*, 157–180.

Ziegler, W., & Weddige, K. (1999). Zur Biologie, Taxonomie und Chronologie der Conodonten. *Paläontologische Zeitschrift, 73*, 1–38.

Publisher's note Springer Nature remains neutral with regard to jurisdictional claims in published maps and institutional affiliations.